

Gyromagnetic Ratios of the 2^+ States in Even Tungsten Isotopes*

G. GOLDRING AND Z. VAGER

Department of Physics, The Weizmann Institute of Science, Rehovoth, Israel

(Received February 21, 1962)

Precession measurements of gyromagnetic ratios have been carried out for the 2^+ states in even tungsten isotopes. The nuclei were excited by Coulomb excitation with a neutral atomic-hydrogen beam and the time-integrated rotation of the angular distribution of the de-excitation gamma rays in an applied magnetic field was measured. The targets were in metal form and the angular distributions were found to be almost unperturbed. The measured gyromagnetic ratios are: $g(W^{182})=0.193\pm 0.018$, $g(W^{184})=0.207\pm 0.016$, and $g(W^{186})=0.292\pm 0.027$. The values obtained for W^{182} and W^{184} are in disagreement with some previous measurements.

I. INTRODUCTION

THE measurement of the gyromagnetic ratios of excited states in even rotational nuclei is of importance because these gyromagnetic ratios are directly related to the pattern of the collective rotational flow. The g factors determine, in effect, the relative contribution of protons and neutrons to the common collective motion. A number of experiments have been carried out in this field in recent years, but the over-all picture is not at all clear and the results are rather inconclusive. To a large extent, this is due to the fact that in many of these experiments the effect of the atomic environment on the nucleus was insufficiently known or understood to allow for an unambiguous determination of the g factors.

The nucleus is, in general, affected by electric and magnetic fields that interact with the nuclear electric quadrupole and magnetic dipole moments and change the nuclear orientation. Such interactions are usually detected by the perturbation of the angular distribution of the decay radiation from the excited nuclear state. The perturbation will always be small if the hyperfine splitting is small compared to the width of the nuclear level. If the field at the nucleus is fluctuating sufficiently rapidly in time even a strong hyperfine interaction may not change the nuclear orientation appreciably.¹ In this case, however, strong magnetic hyperfine interactions may still have an important effect on precession measurements, because the applied magnetic field polarizes the electronic states and the fluctuating magnetic fields will consequently not average to zero.²

The nuclear magnetic moment is then acted on by an effective magnetic field in the direction of the applied field but of different magnitude. The ratio of effective field to applied field may differ considerably from unity for the strongly paramagnetic rare-earth ions. In principle, this ratio may be calculated if the electronic state during the nuclear lifetime and the temperature of the immediate nuclear environment are known. In practice, such calculations and corrections always intro-

duce a certain degree of ambiguity, especially in cases where the corrections are large.

In the present experiment an attempt was made to minimize the effects of hyperfine fields in order to achieve a clear and unequivocal measurement. Precession measurements were carried out for the 2^+ states in even tungsten isotopes by observing the shift in an external magnetic field of the angular distribution of gamma rays following the Coulomb excitation of the 2^+ states. The targets were in metallic form, and the angular distributions were found to exhibit almost no perturbation. Tungsten was chosen for this measurement because it is only very weakly paramagnetic and no induced magnetic fields need to be considered. The conditions of the experiments were therefore such that the motion of the nuclei in the 2^+ state could be attributed solely to the interaction of the nuclear magnetic moment with the applied external magnetic field.

II. NUCLEAR PRECESSION IN SOLID TARGETS

The angular distribution around the particle beam of gamma rays following Coulomb excitation of a 2^+ state is given by³

$$W(\theta) = 1 + A_2 P_2(\cos\theta) + A_4 P_4(\cos\theta), \quad (1)$$

provided the nuclei remain unperturbed for the lifetime of the excited state. A_2 and A_4 are given in reference 3 as

$$A_2 = 0.3571 a_2^{E2}(\eta_i; \xi), \quad A_4 = 1.143 a_4^{E2}(\eta_i; \xi),$$

and $a_2^{E2}(\eta_i; \xi)$, $a_4^{E2}(\eta_i; \xi)$ are tabulated in the same article. In the experiments reported here A_4 was always small. If an external magnetic field H is applied perpendicular to the particle beam, the nuclei, and with them the angular distribution pattern, precess with angular frequency $\omega_H = g\mu_N H/\hbar$ around the field. Here g is the gyromagnetic ratio of the excited state and μ_N the nuclear magneton. If for a state of mean life τ , $\omega_H \tau \ll 1$, the angular distribution averaged over all nuclear lifetimes is given by

$$W_H(\theta) = W(\theta - \omega_H \tau), \quad (2)$$

and the change in the counting rate with and without

* Supported in part by a grant from Harry Scherman, New York.

¹ A. Abragam and R. V. Pound, Phys. Rev. **92**, 943 (1953).

² G. Goldring and R. P. Scharenberg, Phys. Rev. **110**, 701 (1958).

³ K. Alder, A. Bohr, T. Huus, B. Mottelson, and A. Winther, Revs. Modern Phys. **28**, 432 (1956).

field— $n(\uparrow)$ and $n(0)$, respectively—in a counter situated at an angle θ is given by

$$\begin{aligned} \epsilon_p(\theta) &= \frac{n(\uparrow) - n(0)}{n(0)} = -(\omega_H \tau) \frac{1}{W} \frac{dW}{d\theta} \\ &= -\frac{g\mu_N H}{\hbar} \tau \frac{1}{W} \frac{dW}{d\theta} \quad (3) \end{aligned}$$

(for unperturbed targets).

Here \uparrow defines the positive direction of H . If the nuclei in the excited state interact with atomic fields, the angular distribution (1) is modified. If in particular the atomic fields have no preferred axis in space (e.g., in liquids or in microcrystalline solids), we get instead of (1):

$$W'(\theta) = 1 + G_2 A_2 P_2(\cos\theta) + G_4 A_4 P_4(\cos\theta), \quad (4)$$

where G_2 , G_4 are the so-called attenuation coefficients, and $G_2 \leq 1$, $G_4 \leq 1$.

We now consider the motion of nuclei under the combined action of an external magnetic field and static electric fields of atomic origin in randomly oriented microcrystalline surroundings. In keeping with our experimental conditions we shall consider, in particular, time averages over nuclear lifetimes. The nuclei in the excited state can be described by a density matrix $\rho(t)$ which evolves in time according to the equation

$$d\rho/dt = (i/\hbar)[\rho, \mathfrak{H}],$$

where $\mathfrak{H} = \mathfrak{H}_H + \mathfrak{H}_Q$. \mathfrak{H}_H represents the interaction of the nuclei with the external magnetic field, and \mathfrak{H}_Q the interaction with the quadrupole electric field. We write ρ_τ for the time average of $\rho(t)$:

$$\begin{aligned} \rho_\tau &= \frac{1}{\tau} \int_0^\infty e^{-t/\tau} \rho(t) dt = \rho(0) + \int_0^\infty e^{-t/\tau} \frac{d\rho}{dt} dt \\ &= \rho(0) + \frac{i}{\hbar} \int_0^\infty e^{-t/\tau} [\rho, \mathfrak{H}] dt \\ &= \rho(0) + \frac{i}{\hbar} \left[\int_0^\infty e^{-t/\tau} \rho(t) dt, \mathfrak{H} \right] \end{aligned}$$

and therefore,

$$\rho_\tau = \rho(0) + (i/\hbar)\tau[\rho_\tau, \mathfrak{H}]. \quad (5)$$

If, in particular, there is no quadrupole perturbation, we get

$$\rho_\tau^H = \rho(0) + (i/\hbar)\tau[\rho_\tau^H, \mathfrak{H}_H], \quad \mathfrak{H}_Q = 0. \quad (6)$$

This relation between $\rho(0)$ and ρ_τ^H is equivalent to the relation between $W(\theta)$ and $W_H(\theta)$ in (2).

In a similar manner we get for ρ_τ^Q , the density matrix which determines the angular distribution without magnetic field:

$$\rho_\tau^Q = \rho(0) + (i/\hbar)\tau[\rho_\tau^Q, \mathfrak{H}_Q], \quad \mathfrak{H}_H = 0, \quad (7)$$

and after averaging over all orientations of the crystal-

line field:

$$\langle \rho_\tau^Q \rangle_{\text{av}} = \rho(0) + (i/\hbar)\tau \langle [\rho_\tau^Q, \mathfrak{H}_Q] \rangle_{\text{av}}, \quad \mathfrak{H}_H = 0. \quad (7')$$

This relation between $\rho(0)$ and $\langle \rho_\tau^Q \rangle_{\text{av}}$ is equivalent to the relation between $W(\theta)$ and $W'(\theta)$ in (1) and (4).

Finally, we have for ρ_τ in the general case when neither \mathfrak{H}_Q nor \mathfrak{H}_H vanish:

$$\begin{aligned} \rho_\tau &= \rho(0) + (i/\hbar)\tau[\rho_\tau, \mathfrak{H}_H] + (i/\hbar)\tau[\rho_\tau, \mathfrak{H}_Q], \\ \rho_\tau &= \rho_\tau^Q + (i/\hbar)\tau[\rho_\tau, \mathfrak{H}_H] + (i/\hbar)\tau[\rho_\tau - \rho_\tau^Q, \mathfrak{H}_Q], \quad (8) \end{aligned}$$

and averaging over angles:

$$\begin{aligned} \langle \rho_\tau \rangle_{\text{av}} &= \langle \rho_\tau^Q \rangle_{\text{av}} + (i/\hbar)\tau \langle [\rho_\tau]_{\text{av}}, \mathfrak{H}_H \rangle \\ &\quad + (i/\hbar)\tau \langle [\rho_\tau - \rho_\tau^Q, \mathfrak{H}_Q] \rangle_{\text{av}}. \quad (8') \end{aligned}$$

If the magnetic and quadrupole hyperfine splittings $\hbar\omega_H$, $\hbar\omega_Q$ are small so that $\omega_H\tau \ll 1$, $\omega_Q\tau \ll 1$, then one finds that the three terms in (8') are of decreasing orders of magnitude: 1, $(\omega_H\tau)$, $(\omega_H\tau)(\omega_Q\tau)^2$.

If one now evaluates Eq. (8') up to first order in the precession angles, one gets for $\langle \rho_\tau^Q \rangle_{\text{av}}$ the relation (6). This is understandable since $\langle \rho_\tau^Q \rangle_{\text{av}}$ in (7') has no first-order terms (they vanish in the angular integration) and the effects of the quadrupole perturbation appear only in second order. In order to get the leading term of the quadrupole perturbation, we have to evaluate (8') consistently to second order in $(\omega_Q\tau)^2$, and we therefore have to calculate the leading term of

$$(i/\hbar)\tau \langle [\rho_\tau - \rho_\tau^Q, \mathfrak{H}_Q] \rangle_{\text{av}}.$$

From (8) and (6) we get

$$\begin{aligned} (i/\hbar)\tau \langle [\rho_\tau - \rho_\tau^Q, \mathfrak{H}_Q] \rangle_{\text{av}} \\ \sim \{ (i/\hbar)\tau \}^3 \langle [[[\rho(0), \mathfrak{H}_Q], \mathfrak{H}_H], \mathfrak{H}_Q] \rangle_{\text{av}} \\ + \{ (i/\hbar)\tau \}^3 \langle [[[\rho(0), \mathfrak{H}_H], \mathfrak{H}_Q], \mathfrak{H}_Q] \rangle_{\text{av}} \quad (9) \end{aligned}$$

with lower terms dropping out in the angular integration.

It is convenient to decompose $\rho(0)$ in the following manner:

$$\rho(0) = (1/5)I + \rho_{A_2} + \rho_{A_4},$$

where I is the unit matrix, $(1/5)I + \rho_{A_2}$ is a matrix that leads to an angular distribution $W(\theta) = 1 + A_2 P_2(\cos\theta)$, and ρ_{A_4} is defined in an analogous manner.

We write $\hbar\omega_H I_x$ for \mathfrak{H}_H and $\hbar\omega_Q I_x^2$ for the nonscalar part of \mathfrak{H}_Q , with the particle beam along the z axis. Averaging over all directions x' , we get

$$\begin{aligned} (i/\hbar)\tau \langle [\rho_\tau - \rho_\tau^Q, \mathfrak{H}_Q] \rangle_{\text{av}} \\ = -(\omega_Q\tau)^2 (i/\hbar)\tau [12.2\rho_{A_2} + 6.6\rho_{A_4}, \mathfrak{H}_H]. \end{aligned}$$

Inserting this into (8'), we get

$$\begin{aligned} \langle \rho_\tau \rangle_{\text{av}} &= \langle \rho_\tau^Q \rangle_{\text{av}} - (\omega_Q\tau)^2 (i/\hbar)\tau [12.2\rho_{A_2} + 6.6\rho_{A_4}, \mathfrak{H}_H] \\ &\quad + (i/\hbar)\tau \langle [\rho_\tau]_{\text{av}}, \mathfrak{H}_H \rangle. \quad (10) \end{aligned}$$

We now consider the interpretation of Eq. (10). If $A_4 = 0$, the matrix $12.2\rho_{A_2} + 6.6\rho_{A_4}$ in the commu-

tator can be replaced by $12.2\rho(0)$ and to the same order also by $12.2\rho_\tau$. We then get

$$\langle \rho_\tau \rangle_{\text{av}} = \langle \rho_\tau^Q \rangle_{\text{av}} + (i/\hbar)\tau[\langle \rho_\tau \rangle_{\text{av}}, \mathfrak{I}\mathcal{C}_H\{1 - 12.2(\omega_Q\tau)^2\}], \quad A_4 = 0.$$

In reference 1 the attenuation coefficient G_2 is given as $1 - 6.8(\omega_Q\tau)^2$ to second order, and we can therefore write

$$\langle \rho_\tau \rangle_{\text{av}} = \langle \rho_\tau^Q \rangle_{\text{av}} + (i/\hbar)\tau[\langle \rho_\tau \rangle_{\text{av}}, \mathfrak{I}\mathcal{C}_H G_2^{1.8}], \quad A_4 = 0. \quad (11)$$

Comparing this with (6) and (7) we see that the process may be interpreted as a free precession in a field $HG_2^{1.8}$ by the ensemble characterized by $\langle \rho_\tau^Q \rangle_{\text{av}}$. According to (7') this is the ensemble giving rise to the perturbed distribution $W'(\theta)$ as given in (4)—the “experimental” distribution. We can therefore evaluate the change in counting rate ϵ_p with and without field in a target perturbed by quadrupole interactions by replacing $W(\theta)$ in Eq. (3) by $W'(\theta)$ and H by $HG_2^{1.8}$:

$$\epsilon_p(\theta) = -\frac{g\mu_N H}{\hbar} X_2 \tau \frac{1}{W'} \frac{dW'}{d\theta}, \quad X_2 = G_2^{1.8}; \quad A_4 = 0. \quad (12)$$

If $A_2 = 0$ a relation similar to (12) applies with

$$X_4 = G_4^{1.65}; \quad A_2 = 0. \quad (12')$$

In the general case when neither A_2 nor A_4 vanish, the time integrated angular distribution in a magnetic field may be written as

$$W_H'(\theta) = 1 + G_2 A_2 P_2(\cos(\theta - X_2 \omega_H \tau)) + G_4 A_4 P_4(\cos(\theta - X_4 \omega_H \tau)). \quad (12'')$$

(12'') may be compared with a similar relation for liquid targets.¹ For small angles of rotation ($\omega_H \tau \ll 1$) one finds in that case:

$$X_k = G_k \quad (\text{for liquids}). \quad (12''')$$

The relation (12''') is a direct consequence of the fact that in liquids the motion of the nuclei in the magnetic field is independent of the motion in the quadrupole field so that

$$W_H(\theta, t) = 1 + \sum G_k(t) A_k P_k(\cos(\theta - \omega_H t)).$$

So far, we have only considered perturbations of a fixed frequency ω_Q . In practice, one usually expects to get a range of frequencies, especially in states excited by nuclear reactions, since the recoil motion usually dislocates the nuclei from the normal lattice sites, and the quadrupole fields acting on different nuclei may differ considerably. Under such general conditions the X_k are not determined uniquely by the attenuation coefficient, and this is one of the serious drawbacks of precession measurements with perturbed targets (or sources). One can, however, show that the values given in (12) and (12') represent the minimum values of X_k for given G_k .

We consider a frequency spectrum $A(\omega)$, $\int A(\omega) d\omega = 1$, and we have

$$G_k = \int G_k(\omega) A(\omega) d\omega,$$

where $G_k(\omega)$ is assumed to be a known function and

$$X_k = \frac{1}{G_k} \int G_k^n(\omega) A(\omega) d\omega,$$

where $n-1$ may be either one of the exponents in (12) and (12'). We wish to minimize X_k for given G_k , i.e., to find the minimum of $\int [G_k^n(\omega) - \lambda G_k(\omega)] A(\omega) d\omega$. The integral will be minimized by putting $A(\omega) = \delta(\omega - \omega_0(\lambda))$, where $\omega_0(\lambda)$ is the frequency for which $G_k^n(\omega_0(\lambda)) - \lambda G_k(\omega_0(\lambda))$ is a minimum, and λ is fixed by the auxiliary condition $G_k = G_k(\omega_0(\lambda))$. The single frequency spectrum therefore yields the lowest X_k for a given G_k . Since for given G_k the X_k values for static quadrupole fields (12) and (12') are always smaller than the corresponding values for liquid surroundings (12'''), the X_k value computed according to (12) or (12') will have the lowest possible value even if both static quadrupole perturbations and fast relaxation perturbations are considered as possible.

As the frequency spectrum broadens, the value of X_k for a given G_k increases, and under certain circumstances X_k may attain the maximum possible value of unity. Such is the case for example in the perturbation mechanism considered by Kegel⁴ where most of the nuclei were assumed to be essentially unperturbed (i.e., $\omega \rightarrow 0$), whereas a small fraction, say α , are strongly perturbed by a fast process which effectively reduces the anisotropy to zero. In this case: $G_k = 1 - \alpha$ and $X_k = 1$.

If no information on the details of the perturbation mechanism is available, apart from the knowledge of G_k , one can therefore assume knowledge of X_k only to within the limits given above. In the present experiment, we take for X_2 the value

$$\dot{X}_2 = (1/2)[(1 + G_2^{1.8}) \pm (1 - G_2^{1.8})], \quad 1 - G_2 \ll 1. \quad (13)$$

Since A_4 is small, the difference between X_2 and X_4 may be ignored, and Eq. (12) is adequate for these measurements.

III. ANGULAR DISTRIBUTION MEASUREMENTS

The tungsten targets were prepared by the following procedure: Isotopically pure tungsten oxide was reduced to metal in a hydrogen atmosphere of 800 to 900°C. Some 40 mg of the metallic powder were pressed into a disk of 5-mm diameter and were heated first in a hydrogen atmosphere to about 900° and then in vacuum to about 2000°C.

⁴ G. H. R. Kegel, thesis, Massachusetts Institute of Technology, 1961 (unpublished).

Angular distribution measurements of gamma rays following Coulomb excitation were carried out at two proton energies: 1.4 and 2.0 MeV. The first is the energy at which the precession measurements were carried out and the second was chosen because at that energy A_4 is almost exactly zero for all three tungsten isotopes and the analysis of the measurements is therefore facilitated. The proton bombardment energies were calibrated against the $\text{Li}^7(p,n)$ threshold at 1.881 MeV. As an independent check on the energy, the yield of gamma rays from the tungsten targets was also measured. This measurement has the merit that one actually determines the energy of the protons as they strike the tungsten, even if there is some film or deposit on the surface of the target. Gamma-ray yields were measured at 1.4 and 2.0 MeV for all three isotopes and all were within seven percent of the values calculated from measured $B(E2)$ values.⁵ In Fig. 1 the coefficient A_2 is shown plotted against the gamma-ray yield as calculated for a thick W^{184} target. The measured yield values at 1.4 and 2.0 MeV are also shown against the values $A_2(E_0)$ corresponding to these energies. It is clear from this figure that if one uses the function $A_2(Y)$ to determine the A_2 values for the tungsten targets from the measured yields, these values will be very close to the nominal value $A_2(E_0)$.

The angular distribution measurements were carried out with an NaI scintillation crystal $1\frac{1}{4}$ in. in diameter and $\frac{1}{4}$ in. thick, bonded to a type 6810 photomultiplier. The crystal was placed at a distance of 55 mm from the target and the solid angle of the counter was determined by a 30-mm diameter opening in a 5-mm-thick lead sheet in front of the crystal. A tin absorber with areal density 70 mg/cm² was placed in front of the counter

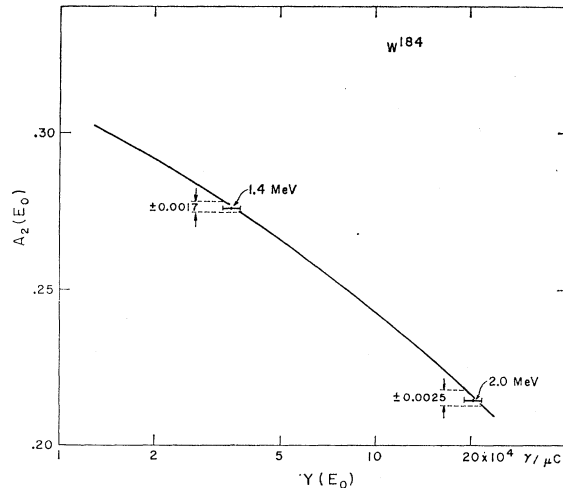


FIG. 1. The coefficient A_2 as a function of the gamma-ray yield as calculated for a thick W^{184} target. The measured yield values are shown against the A_2 value corresponding to the energy of the bombarding protons.

⁵ O. Hansen, M. C. Olesen, O. Skilbreid, and B. Elbek, Nuclear Phys. 25, 634 (1961).

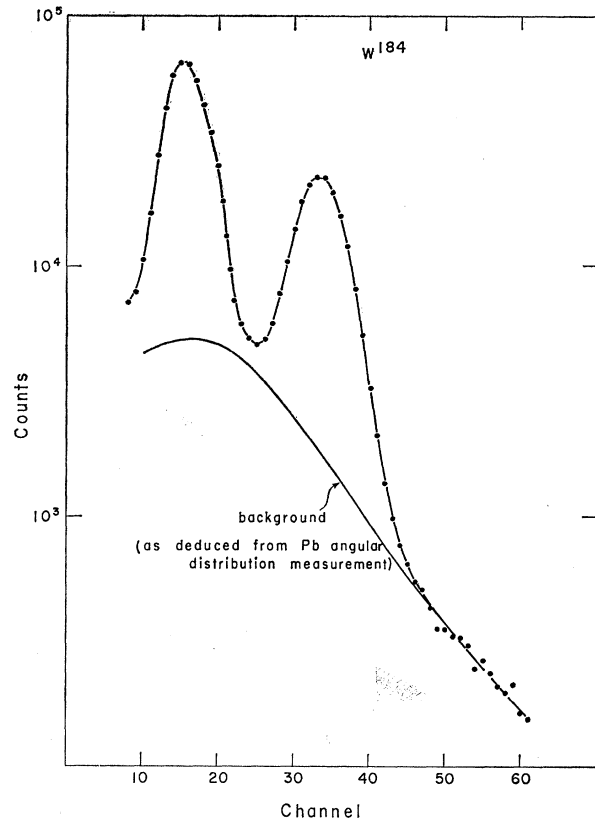


FIG. 2. Gamma-ray spectrum from W^{184} bombarded by protons of 1.4 MeV in an angular distribution measurement.

in order to decrease the intensity of the K x rays from the target. A typical gamma-ray spectrum is shown in Fig. 2. The angular distribution of the gamma rays was determined by recording the ratio of gamma rays to K x rays (which are isotropic) at different angles.

The general background encountered in these measurements was almost entirely due to proton bremsstrahlung, and it contributed between 6 and 10% to the gamma-ray and x-ray counts. A detailed study of the background radiation was carried out with the aid of a lead target. The angular distribution of photons of different energy emitted from the lead target was measured and compared to the calculated bremsstrahlung distribution.³ The average ratio of the measured coefficient A_2 to the calculated value was found to be 1.05 ± 0.15 . Similar results were obtained for photons of high energy (beyond the Coulomb-excited gamma rays) from the tungsten targets. On the strength of these measurements the contribution of the background radiation to the angular distributions could be established accurately and reliably from the measured spectrum of gamma rays from lead and the computed bremsstrahlung distribution coefficients.³ In practice, the contributions of the background angular distribution to the gamma rays and to the x rays were found to be very nearly equal so that they almost cancel each other. The

TABLE I. Results of angular distribution measurements at 2- and at 1.4-MeV bombarding energy. At 2 MeV the angular distribution is given by: $W(\theta)=1+G_2A_2P_2(\cos\theta)$ and at 1.4 MeV by $W(\theta)=1+G_2A_2P_2(\cos\theta)+A_4P_4(\cos\theta)$. The justification for setting $G_4=1$ is discussed in the text. The measurements marked by (a) were carried out after the precession measurements in the order indicated by the numerals. The measurement marked by (b) was carried out before the precession measurement. The measurements marked by stars are preliminary measurements ("old" targets) and are given for comparison.

| Nucleus | Calculated A_2, A_4 | | | Measured G_2 | | Mean value |
|-------------------|-----------------------|-----------------|-----------------|----------------------------|---|-------------|
| | A_2 (2.0 MeV) | A_2 (1.4 MeV) | A_4 (1.4 MeV) | at 2.0 MeV | at 1.4 MeV | |
| W ¹⁸² | 0.2018 | 0.2632 | -0.0353 | 0.930±0.035 ^(a) | 0.925±0.065 ^(a) | 0.925±0.030 |
| W ¹⁸⁴ | 0.2144 | 0.2757 | -0.0452 | 0.940±0.065 ^(a) | $\left\{ \begin{array}{l} 0.940\pm 0.035^{(b)} \\ 0.995\pm 0.030^{(a_1)} \\ 0.885\pm 0.025^{(a_2)} \end{array} \right.$ | 0.940±0.015 |
| W ¹⁸⁶ | 0.2279 | 0.2871 | -0.0551 | 0.980±0.050 ^(a) | 0.925±0.030 ^(a) | 0.940±0.025 |
| W ^{182*} | | 0.2632 | -0.0353 | | 0.935±0.085 | 0.94 ±0.08 |
| W ^{184*} | | 0.2757 | -0.0452 | | $\left\{ \begin{array}{l} 1.070\pm 0.065 \\ 1.015\pm 0.060 \end{array} \right.$ | 1.04 ±0.05 |
| W ^{186*} | | 0.2871 | -0.0551 | | 0.975±0.060 | 0.98 ±0.06 |
| Sm ¹⁵² | | 0.2714 | -0.040 | | 0.635±0.045 | 0.635±0.045 |

results are therefore less sensitive to the angular distribution of the background radiation than would be the case in an angular distribution measurement of the gamma rays normalized to the total charge falling on the target.

As a general check the angular distribution of the 137-keV radiation from Ta¹⁸¹ was measured. This radiation is emitted from a short-lived state and its distribution is well known and nearly isotropic. The measured distribution was found to be consistent with a mixing ratio: $\delta = (E2/M1)^{1/2} = + (0.2)^{1/2}$, which represents the mean value of all the available information and seems to be well substantiated. Actually the computed angular distribution does not depend very much on δ^2 but the sign of δ is important, and our measurement of the angular distribution is definitely in agreement only with a positive value of δ .

The angular distribution of the 110-keV radiation from W¹⁸⁴ excited with protons of 1.4 MeV is shown in Fig. 3 as a general illustration.

The angular distribution measurements were corrected for the finite aperture of the counter, for multiple scattering of the beam in the target—this amounted to a correction of about 3 to 5% in G_2 and 15 to 17% in G_4 —and for absorption of the radiation in the target material. The last correction was found to be practically negligible. The angular distribution of gamma rays from a perturbed target is given in (4). At 2-MeV bombarding energy the parameter A_4 very nearly vanishes and the measurements therefore determine the sole parameter G_2 .

At 1.4-MeV bombarding energy both G_2 and G_4 should, in principle, be determined from the measurements. However, since A_4 is small and since the angular distributions were found to be almost unperturbed, G_4 was arbitrarily set equal to unity and only G_2 was determined from the measurements. This treatment of the P_4 term introduces only a negligible error into the evaluation of the X coefficients and the precession measurements.

The results of the angular distribution measurements are given in Table I. Also given in this table are results of some earlier measurements that were carried out with targets prepared in a somewhat different way: These

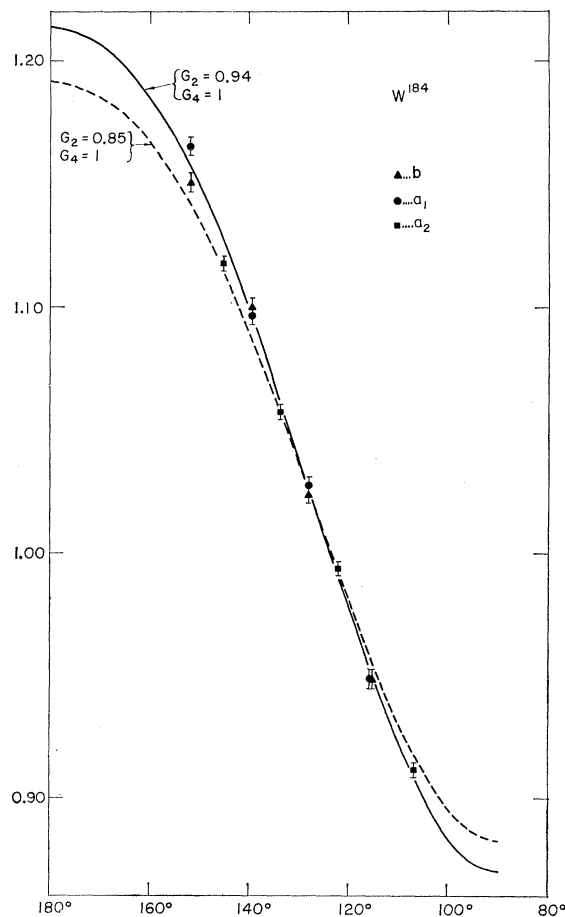


Fig. 3. Angular distribution of 110-keV gamma rays following Coulomb excitation of W¹⁸⁴ with protons of 1.4 MeV. The three individual measurements b, a_1, a_2 are also referred to in Table I.

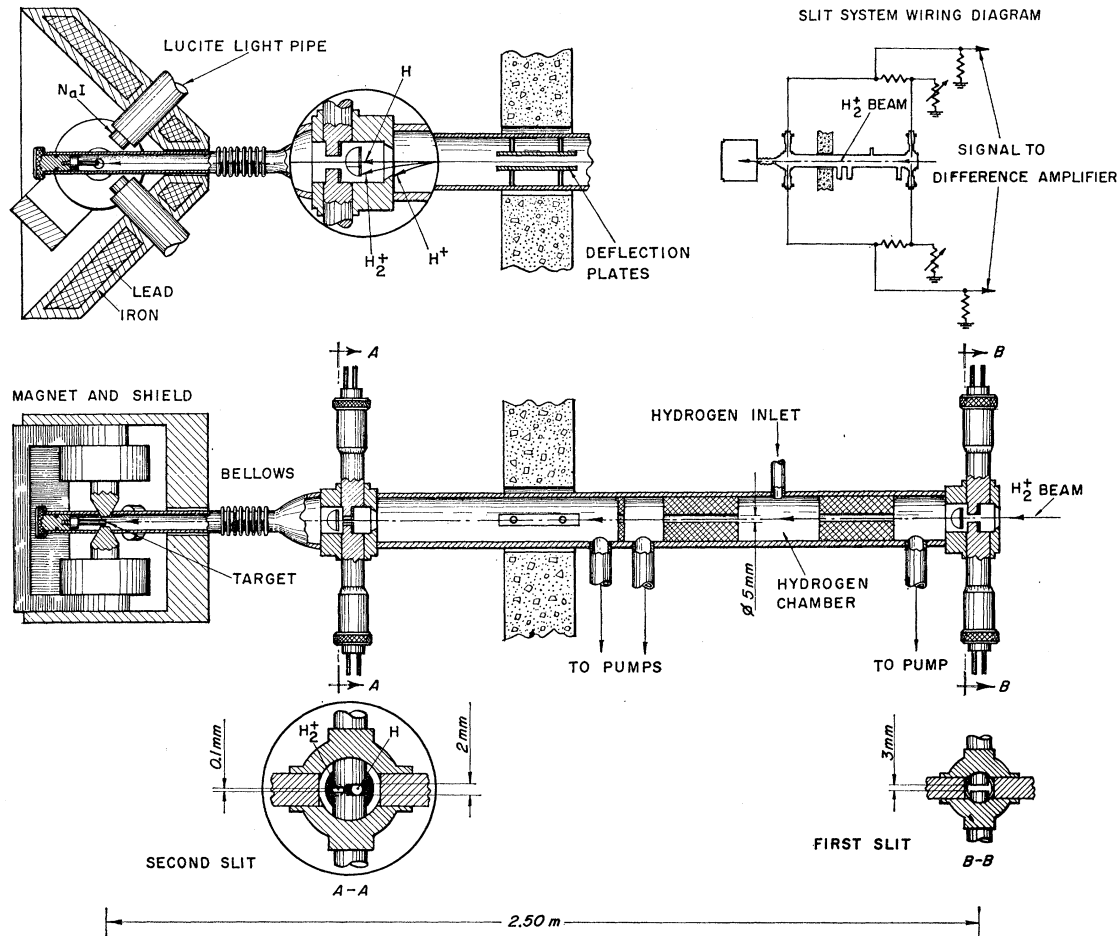


FIG. 4. Schematic view of the magnet, the counters, and the arrangement used for producing a neutral hydrogen beam.

“old” targets were fixed onto a support with an organic glue. The glue rose through cracks in the target material to the surface and gave rise to some background radiation which made the analysis of the measurement more difficult and the results less accurate. In contrast to these “old” targets, the “new” targets were simply pressed against the support with a thin copper ring. Measurements with a Sm_2O_3 target containing Sm^{152} are also summarized in Table I. The G_2 value found for this radiation is in good agreement with earlier measurements.²

There was some indication that targets deteriorate (G_2 decreases) with time or after long runs. The precession measurement (taking about eight hours) was therefore carried out immediately after preparation of the target, and the angular distribution was measured last. In one case, W^{184} , angular-distribution measurements were carried out both before and after the precession measurement. As may be seen from Table I, no significant change in the target can be detected.

The G_2 values measured at 2.0- and 1.4-MeV bombarding energies agree very well. This seems particularly significant since the experimental conditions

(counting rate, ratio of gamma to x-ray counts, anisotropy) were quite different for the two cases. The G_2 value for W^{182} also agrees very well with the differential angular distribution measurements of Kegel.⁴

IV. PRECESSION MEASUREMENTS

(a) General

The precession measurements were carried out in the customary arrangement of two fixed counters at $\pm 135^\circ$ to the particle beam and a magnetic field perpendicular to the plane of the counters.² A schematic view of the magnet and the counters is shown in Fig. 4. The magnetic field was produced by a small electromagnet with a gap 5 mm wide and 5 mm in diameter, and the field at the center of the gap was measured with a flip coil as 20.3 ± 0.2 kG. The field was also measured and mapped with a Hall-effect probe. The gamma counters were 1-in. diam by $\frac{1}{2}$ -in. thick NaI scintillation crystals bonded to 4.5-in.-long Lucite light guides and EMI 9558B photomultipliers. The photomultipliers were shielded from strong magnetic fields by a double-walled iron box encasing the magnet. This box also served

as a container for lead for shielding against stray gamma radiation.

The precession of an excited nucleus in the applied field causes a change in the intensity of the de-excitation radiation reaching the counters. In the counter at $+135^\circ$ the change in counting rate is given according to (3) or (12):

$$n_1(\uparrow)/n_1(0) = 1 + \epsilon_p(+135^\circ) = 1 + \epsilon_p.$$

In the other counter the ratio will be

$$n_2(\uparrow)/n_2(0) = 1 + \epsilon_p(-135^\circ) = 1 - \epsilon_p,$$

so that the ratio of counts in the two counters is given by

$$R(\uparrow) = \frac{n_1(\uparrow)}{n_2(\uparrow)} \div \frac{n_1(0)}{n_2(0)} = \frac{1 + \epsilon_p}{1 - \epsilon_p}.$$

Similarly, if the field is reversed,

$$R(\downarrow) = (1 - \epsilon_p)/(1 + \epsilon_p),$$

and therefore

$$\frac{R(\uparrow)}{R(\downarrow)} = \frac{n_1(\uparrow)}{n_2(\uparrow)} \div \frac{n_1(\downarrow)}{n_2(\downarrow)} = \left(\frac{1 + \epsilon_p}{1 - \epsilon_p} \right)^2. \quad (14)$$

In precession measurements following excitation by charged particles, the experimentally measured double ratio (14) is often affected not only by the precession of the excited nuclei but also by the action of the field on the beam itself.² The field changes both the angle of incidence and the point of impact of the beam on the target, and in experiments involving nuclear states with mean lives of 2×10^{-9} sec or less, the resulting changes in counting rate in the detectors may well surpass the effects due to precession.

In the present experiment this difficulty was overcome by bombarding the target with a neutral beam of hydrogen atoms which gets ionized immediately upon impact on the target. The atomic beam was produced by the well-known method of passing high-energy molecular hydrogen ions through a gas chamber. Some of the molecular ions are broken into protons and hydrogen atoms and the charged beams are filtered out by electrostatic fields.

b. The Neutral Hydrogen Beam

The details of the experimental arrangement are shown in Fig. 4: H_2^+ ions after being accelerated to 2.8 MeV in a Van de Graaff accelerator and deflected through 90° in a deflection magnet, pass through an energy-defining slit and then through a hydrogen chamber which is differentially pumped on both sides. A mixed beam of H_2^+ , H^+ , and H emerges from the chamber, and the charged particles are deflected out of the way by an electrostatic field. The protons and the hydrogen atoms have an energy of 1.4 MeV. The neutral H beam passes through a defining slit and onto the

target which is situated between the pole tips of the magnet.

Three types of molecular reactions occur in the hydrogen chamber:

- (1) the break-up reaction: $H_2^+ \rightarrow H^+ + H$;
- (2) the ionization of the molecular ions: $H_2^+ \rightarrow 2H^+ + e^-$;
- (3) the ionization of the hydrogen atoms: $H \rightarrow H^+ + e^-$.

Let $N_2(z)$, $N_+(z)$, $N_0(z)$ denote the number of the three different types of molecules at a distance z from the entrance of the hydrogen chamber. We introduce the quantities $\chi_2 = \sigma_2/\sigma_1$, $\chi_3 = \sigma_3/\sigma_1$, where σ_1 , σ_2 , and σ_3 stand for the respective reaction cross sections, and we describe the evolution of the different beams inside the hydrogen chamber by the relations:

$$\begin{aligned} dN_2(x) &= -(1 + \chi_2)N_2(x)dx, \\ dN_0(x) &= N_2(x)dx - \chi_3N_0(x)dx, \\ dN_+(x) &= (1 + 2\chi_2)N_2(x)dx + \chi_3N_0(x)dx, \end{aligned} \quad (15)$$

where the coordinate x is measured in units of the mean free path l for the breakup reaction: $x = z/l$. Equations (15) are compatible with the conservation of the number of protons:

$$2N_2(x) + N_0(x) + N_+(x) = 2N_2(0).$$

The available information on the cross sections here considered is not sufficient for an accurate evaluation of (15). In order to get an order of magnitude estimate, we assume all cross sections to be equal and we get

$$N_0(x) = N_2(0)(e^{-x} - e^{-2x}).$$

This function has a maximum at the point

$$x_{\max} = \log_e 2, \quad (16)$$

and the maximum value $N_0(x_{\max})$ is given by

$$N_0(x_{\max}) = (1/4)N_2(0). \quad (17)$$

In our experiment $N_0(x)$ was maximized empirically by varying the pressure of the gas in the chamber. The maximum ratio $N_0(x_{\max})/N_2(0)$ was found to be close to 10% which agrees reasonably well with the very rough estimate in Eq. (17). The value $z_{\max} = lx_{\max}$ was found to be very roughly 1 (cm \times mm Hg), which according to (16) would imply $l \sim 2$ (cm \times mm Hg). Direct measurements of σ_3 have been reported for proton energies up to 1 MeV.⁶ Extrapolating these measurements to 1.4 MeV one gets: $\sigma_3 \sim 10^{-17}$ cm²/atom and for the mean free path $l \sim 1.5$ (cm \times mm Hg).

In order to maximize the H beam actually hitting the target, one should have the focal spot of the H_2^+ beam (the image point of the ion source) as close as possible to the target. On the other hand, for large *total* currents one has to have the focal spot at the energy defining

⁶ C. F. Barnett and H. K. Reynolds, Phys. Rev. **109**, 335 (1958).

slit, as the fractions of the total current falling on the two sides of this slit serve as input signals to a feedback system stabilizing the voltage of the accelerator. Reducing the size of the beam spot on the slit therefore improves the voltage stability and hence the current intensity.

In the present experiment it was therefore found expedient to take the input signal directly from the defining slit ("second slit") in Fig. 4 close to the target. The current falling on this slit is the deflected H_2^+ beam emerging from the hydrogen chamber. The part of the slit exposed to the H_2^+ beam was 0.1-mm wide, whereas the central portion was 2-mm wide, letting the neutral beam through essentially unobstructed. As the H_2^+ beam has to pass through several narrow holes before reaching this slit, the range over which the feedback system can work with this signal is very limited. The usual energy-defining slit ("first slit" in Fig. 4) was therefore also connected to the stabilizer through a resistor chain (upper right-hand corner in Fig. 4) so that it could still exercise some measure of control, although it would not materially interfere with the normal action of the other slit. With this arrangement a stable neutral beam corresponding to one microampere of protons could be produced, with a cross section of $2 \times 2 \text{ mm}^2$ at the target.

The residual gas in the vacuum chamber causes a fraction of the beam to get ionized on its way to the target. This fraction, the contamination of the neutral beam, is given by

$$\nu = N_+/N_0 = \sigma_3'/\sigma_3 = \Delta z/l;$$

here σ_3' is the cross section for the ionization of the hydrogen atoms in the residual gas and Δz corresponds to a path section close to the precession magnet from which charged particles can still reach the target without being deflected off completely by the magnetic field. The length of this section was about 7 cm. We can rewrite the last equation as

$$\nu = (\sigma_3'/\sigma_3) \chi_3 (\Delta z/l),$$

where σ_3 is, as before, the cross section for ionization in the hydrogen. The residual gas in our experiments was mostly gas liberated from the targets under bombardment and consisted presumably of air and organic vapors. For an estimate of σ_3'/σ_3 we take the values of σ_3' , σ_3 given in reference 6 for nitrogen and hydrogen, and get: $\sigma_3'/\sigma_3 \sim 7$. χ_3 we assume, as before, to be of order unity, and for l we take $l = 2$ (cm \times mm Hg). The pressure in the vicinity of the targets was estimated as $1-3 \times 10^{-4}$ mm Hg for the "new" targets. Somewhat higher pressures were encountered when the "old" targets were bombarded, due presumably to outgassing of the glue with which those targets were bonded to the backing. Collecting all the numerical values given above we get as an estimate for the charge contamination of the neutral beam: $\nu \sim 0.01$ (for new targets).

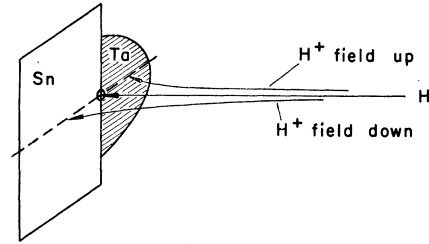


FIG. 5. Special target used for measuring charge contamination of the neutral beam.

The fraction ν was also measured directly with the aid of a specially prepared target shown in Fig. 5. This was a tantalum target of the same size and shape as the regular targets, half of which was covered by a piece of tin. The target was bombarded by the neutral beam and K x rays from Sn and Ta were counted. With the field off the beam is shared about equally between Sn and Ta. When the field is switched on in the direction appropriate to the deflection of protons from Sn to Ta ("field up" in Fig. 5), the Ta receives virtually the total H^+ beam falling on the target at all, and we therefore get for the double ratio of Ta and Sn x rays with and without field:

$$\frac{n(\text{Ta})_H}{n(\text{Sn})_H} : \frac{n(\text{Ta})_0}{n(\text{Sn})_0} = \frac{\frac{1}{2}N_0 + N_+}{\frac{1}{2}N_0} = 1 + 2\nu.$$

ν was measured in this way as

$$\nu = 0.011 \pm 0.005, \quad (18)$$

in good agreement with the estimate given above.

A contamination of the neutral beam of this order is not expected to affect the precession measurements appreciably. It is nevertheless important to analyze in some detail the effects produced by the action of the magnetic field on the charged beam; first, in order to establish the limits on the accuracy of the precession measurements imposed by these effects, and second, because the small spurious effects can be detected and measured directly in nonprecessing radiations—e.g. K x rays or the 137-keV radiation from Ta^{181} —and they afford in this way a sensitive check on the measurements as a whole.

The action of the magnetic field on the charged beam produces two types of spurious effects in the double ratio measurements $R(\uparrow)/R(\downarrow)$.

(a) The shift in the point of incidence on the target changes the solid angle subtended by the counters at the target spot. If we denote by Ω_1 , Ω_2 the solid angles corresponding to the points of incidence with field up and down, respectively, we have

$$R(\uparrow)/R(\downarrow) = \{1 - [(\Omega_2 - \Omega_1)/\Omega_0]\nu\}^2,$$

or, defining a quantity ϵ_Ω by a relation similar to (14):

$$\epsilon_\Omega = \frac{1}{2} [(\Omega_2 - \Omega_1)/\Omega_0]\nu.$$

The quantity $(\Omega_2 - \Omega_1)/\Omega_0$ was estimated from the geometry of the counters and the radial distribution of the magnetic field as $-(0.07 \pm 0.0015)$, and we therefore get from (18):

$$\epsilon_\Omega = -(0.035 \pm 0.007)\nu \sim -(4 \pm 2)10^{-4} \quad (\text{for "new" targets}), \quad (19)$$

with the field directions and counter positions the same as in (14).

(b) The angle of incidence of the charged beam on the target is changed on the average by the amount

$$\Delta\theta = \frac{1}{N_+} \int_0^\zeta \frac{dN_+}{d\zeta'} d\zeta' \int_0^{\zeta'} \frac{H(\zeta'') d\zeta''}{(H\rho)} = \frac{1}{\zeta} \int_0^\zeta d\zeta' \int_0^{\zeta'} \frac{H(\zeta'') d\zeta''}{(H\rho)},$$

where $(H\rho)$ refers to the proton momentum, and ζ (in units of length) corresponds to the quantity Δz defined above.

This was evaluated from the radial distribution of the field as

$$\Delta\theta = 0.11.$$

The rotation of the beam produces a change in counting rate

$$\left(\frac{1}{W_E} \frac{dW_E}{d\theta} \right) \Delta\theta,$$

where $W_E(\theta)$ is the experimentally measured angular distribution. Considering finally counts produced by both the neutral and the charged beam we get for the expected change in counting rate:

$$\epsilon_\theta = 0.11 \left(\frac{1}{W_E} \frac{dW_E}{d\theta} \right) \nu = (12 \pm 6) \left(\frac{1}{W_E} \frac{dW_E}{d\theta} \right) 10^{-4}. \quad (20)$$

The measured double ratio $R(\uparrow)/R(\downarrow)$ generally involves effects due to precession and to the deflection of the charged beam:

$$\epsilon = \epsilon_p + \epsilon_\Omega + \epsilon_\theta.$$

For the angular distribution of gamma rays following excitation of the 2+ levels (including the contribution of the bremsstrahlung), we get

$$(1/W_E) dW_E/d\theta = 0.3 \pm 0.03,$$

and from (19) and (20)

$$\epsilon_\Omega + \epsilon_\theta = 0 \pm 7 \times 10^{-5}.$$

We therefore have

$$\epsilon = \epsilon_p \text{ for } 2^+ \text{ levels}. \quad (21)$$

The error involved in (21) is much smaller than the statistical error in the measurement of ϵ and can therefore be neglected.

Double ratio measurements were also carried out for K x rays and for the gamma rays from the 137-keV level in Ta¹⁸¹. These radiations are all essentially isotropic and we therefore have

$$\epsilon = \epsilon_\Omega \text{ for isotropic radiations}. \quad (22)$$

(c) Details of Measurements

Precession measurements were carried out by reversing the magnetic field every ten seconds and recording the double ratio $R(\uparrow)/R(\downarrow)$ of counts in the two counters for the two field directions in four different parts of a 256-channel analyzer. The effect of the magnetic field on the photomultipliers was tested with a Co⁵⁷ source

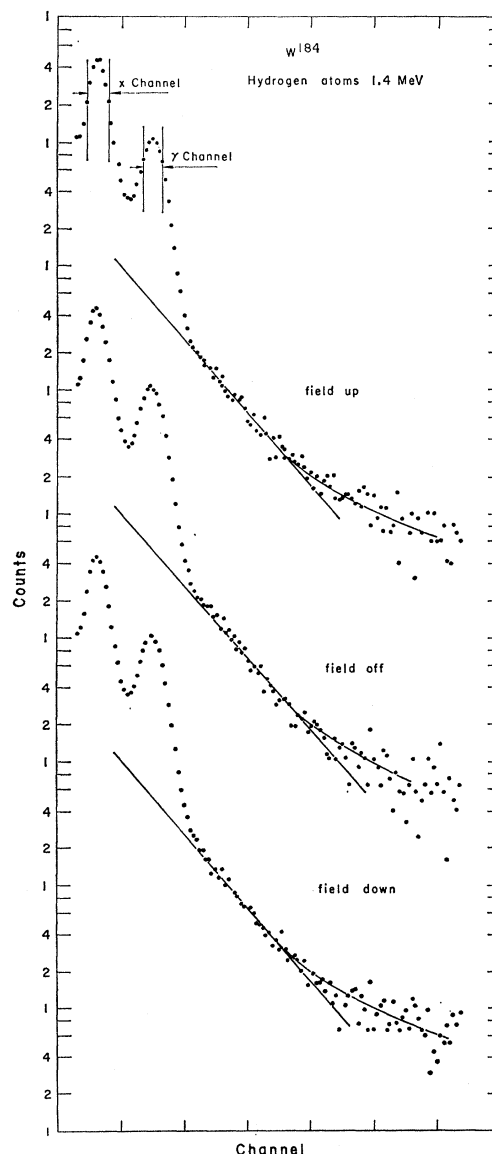


FIG. 6. Gamma spectrum from W¹⁸⁴ in precession measurement, with and without magnetic field, showing that background is low and unaffected by magnetic field.

TABLE II. Results of double ratio measurements. The quantity ϵ is related to the double ratio: $R(\uparrow)/R(\downarrow) = (1+\epsilon)^2/(1-\epsilon)^2$. The errors quoted in the table are the mean deviations derived from the number of counts. ϵ values are given for gamma rays and K x rays.

| Nucleus | Nonprecessing radiation $\epsilon = \epsilon_\Omega$ | | Precessing radiation $\epsilon = \epsilon_p$ |
|-------------------|---|-----------------------|---|
| | $100\epsilon(X)$ | $100\epsilon(\gamma)$ | $100\epsilon(\gamma)$ |
| W ¹⁸² | -0.03±0.02 | | 1.018±0.050 |
| W ¹⁸⁴ | -0.08±0.03 | | 0.998±0.046 |
| W ¹⁸⁶ | -0.07±0.02 | | 1.173±0.057 |
| W ^{182*} | -0.04±0.04 | | 0.97±0.07 |
| W ^{184*} | -0.14±0.04 | | 1.00±0.07 |
| W ^{186*} | -0.13±0.03 | | 1.15±0.06 |
| Ta ¹⁸¹ | -0.10±0.03 | -0.09±0.05 | |
| Sm ¹⁵² | -0.04±0.04 | | 0.80±0.04 |

and was found to be negligible (introducing an error of less than one percent into the precession measurements). Results of double ratio measurements of gamma and K x-ray radiations from the tungsten isotopes, from Sm¹⁵² (in Sm₂O₃) and from Ta¹⁸¹, are summarized in Table II. Results of earlier measurements carried out with the "old" targets of tungsten isotopes are also given in this table for comparison. The values in the last column of

Table II—the actual precession measurements—have been corrected for background by multiplying the measured values by an appropriate factor which depends on the fraction of background counts in the gamma channels and is of the order of 1.08.

The energy spectrum of radiation from a W¹⁸⁴ target is shown in Fig. 6, with the field off, up, and down. It is evident from this figure that no appreciable amount of high-energy radiation is registered in the counters; there is even less of an indication of any difference in this part of the spectrum in the various field positions (as would be expected if for example the charged component of the beam were hitting the target chamber in one particular field position).

Figure 7 presents a complete record of all the individual double ratio measurements carried out with the "new" tungsten targets. The dotted lines give the values for the standard deviations of the individual measurements as computed purely on the basis of counting statistics, whereas the errors quoted for the ϵ values are the standard deviations of the mean values. It is evident from the figure that the scatter of the individual points is random, and that the fluctuations are not significantly larger than the fluctuation due to counting statistics. The combined mean deviation of all points in Fig. 7 about these respective mean values is $|\Delta\epsilon| = 5.5 \times 10^{-4}$, whereas the value computed from the number of counts is $|\Delta\epsilon| = 5.0 \times 10^{-4}$.

The ϵ values for the "nonprecessing" radiations (K x rays and Ta gamma rays) are compatible with the estimate made in (19) and (22) on the basis of the effect of the field on the charged beam component. Combining the results of all measurements with "new" targets, we get

$$\epsilon = (7 \pm 1) \times 10^{-4}$$

for nonprecessing radiations. It is also significant that with the "old" targets larger values of ϵ were found, since the pressure was in these cases consistently higher, and one would therefore also expect a larger degree of charge contamination of the beam.

In accordance with (21) we set

$$\epsilon_p = \epsilon$$

for the precessing radiations, which should be valid irrespective of the fraction of charged beam ν . Significantly, the ϵ values for the precessing radiations in measurements with old and "new" targets are very similar, despite the big difference in the ϵ values for the nonprecessing radiations.

For finite geometry measurements, the relation (12) should be modified to

$$\epsilon = -\frac{g\mu_N H}{\hbar} \tau \left(\frac{1}{W} \frac{dW}{d\theta} \right)_{\Omega_H} X_2, \quad (22)$$

where $[(1/W)dW/d\theta]_{\Omega_H}$ refers to the angular distribution of the precessing radiation as recorded by the

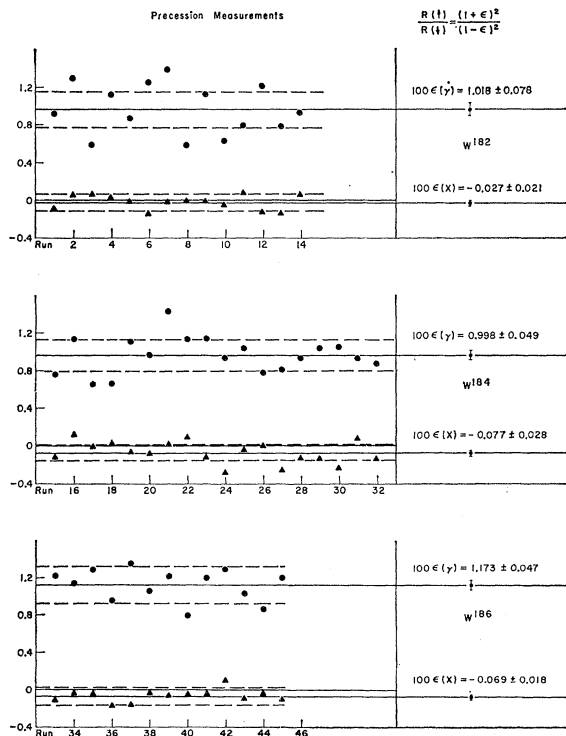


FIG. 7. Summary of double ratio measurements on gamma rays and K x rays from W¹⁸², W¹⁸⁴, W¹⁸⁶ ("new" targets). The dotted lines give the values for the standard deviations of the individual measurements as computed on the basis of counting statistics. The errors quoted for the ϵ values are the standard deviations of the mean values.

TABLE III. Results of precession measurements. The values of ϵ are taken from Table II, and the values of G_2 are taken from Table I. The coefficients X_2 are computed according to Eq. (13).

| Nucleus | 100 ϵ | $\left(\frac{1}{W} \frac{dW}{d\theta}\right)_{\Omega_H}$ | G_2 | X_2 | τ (nsec) | g | from other work |
|-------------------|----------------|--|-------------|-------------|------------------------|-------------|--------------------------|
| W ¹⁸² | 1.018±0.050 | -0.282±0.010 | 0.925±0.030 | 0.935±0.065 | 2.06±0.06 ^a | 0.193±0.018 | 0.404±0.027 ^c |
| W ¹⁸⁴ | 0.998±0.046 | -0.294±0.006 | 0.940±0.015 | 0.945±0.055 | 1.79±0.05 ^a | 0.207±0.016 | 0.38 ±0.05 ^d |
| W ¹⁸⁶ | 1.173±0.057 | -0.300±0.010 | 0.940±0.025 | 0.945±0.055 | 1.46±0.06 ^a | 0.292±0.027 | |
| Sm ¹⁵² | 0.80 ±0.04 | -0.20 ±0.02 | 0.63 ±0.05 | | 2.07±0.07 ^b | | |

$$g = -209.1 \epsilon \left[H_{kG} \tau_{nsec} \left(\frac{1}{W} \frac{dW}{d\theta} \right)_{\Omega_H} X_2 \right]^{-1} \quad H = 20.3 \pm 0.2 \text{ kG}$$

^a See reference 7.
^b See reference 8.
^c See reference 4.
^d See reference 5.

counters used in the precession experiment (including also the effects of multiple scattering of the protons in the target).

For numerical evaluations, (22) is conveniently written as

$$g = -209.1 \epsilon \left[H_{kG} \tau_{nsec} \left(\frac{1}{W} \frac{dW}{d\theta} \right)_{\Omega_H} X_2 \right]^{-1} \quad (23)$$

The ϵ values of the precessing radiations and other data required for the evaluation of the g factors are summarized in Table III. The values of the mean lives τ for the tungsten isotopes were taken from recent measurements in this laboratory,⁷ and the value for Sm¹⁵² was taken from Birk *et al.* and Sunyar.⁸ The tungsten lifetime measurements are in very good agreement with Coulomb-excitation cross-section measurements, and with the measurements of Kegel⁴ for W¹⁸², and Bodenstedt *et al.*⁹ for W¹⁸⁴. The g factors for W¹⁸² and

W¹⁸⁴ as measured in earlier work^{4,9} are also given in the table. There is obviously a severe and unresolved discrepancy between the present results and the results quoted.

The Sm¹⁵² measurement was carried out as a general check. The g factor of the 2+ state of Sm¹⁵² has recently been measured as: $g = 0.375 \pm 0.03$.¹⁰ Interpreting the present results as a measurement of X_2 , we get

$$X_2 = 0.53 \pm 0.04.$$

The dependence of X on $\omega_Q \tau$ or G_2 has been discussed above; however, the relation derived there was only appropriate as a first-order approximation and loses its meaning for G_2 values as low as encountered in this measurement (c.f. Table I). In principle, X_2 could be calculated exactly for all values $\omega_Q \tau$, but such a calculation would not be of great value since the spectral distribution of the perturbation is not known. One can however form a general idea as to the appropriate value of X_2 from the following data: (i) for small perturbations the first-order calculation is valid, and (ii) for large perturbations X_2 assumes small values. Figure 8 summarizes these relations, and it is evident that the value of X_2 found in the present experiment is very reasonable and is certainly not *too low* by a large amount. In terms of ϵ this would mean that the measured value of ϵ seems reasonable, and that if it at all

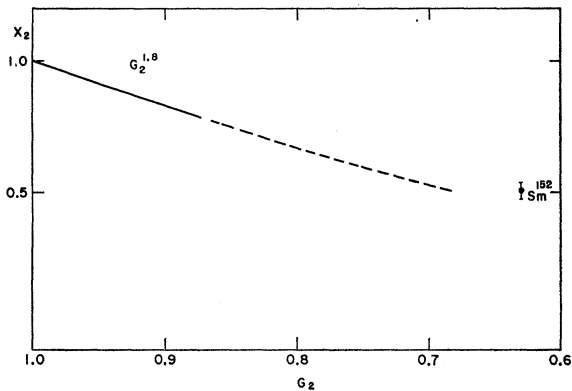


FIG. 8. The coefficient X_2 as function of G_2 , according to the relation $X_2 = G_2^{1.8}$. The full line indicates the expected range of validity of this relation. The measured value of X_2 for the 2+ state in Sm¹⁵² (in Sm₂O₃) is also shown.

⁷ M. Birk, A. E. Blaugrund, G. Goldring, E. Z. Skurnik, and J. S. Sokolowsky, Phys. Rev. **126**, 726 (1962).

⁸ M. Birk, G. Goldring, and Y. Wolfson, Phys. Rev. **116**, 730 (1960); A. W. Sunyar, *ibid.* **98**, 653 (1955).

⁹ E. Bodenstedt, E. Matthias, H. J. Körner, E. Gerdaud, F. Frisius, and D. Hovestadt, Nuclear Phys. **15**, 239 (1960).

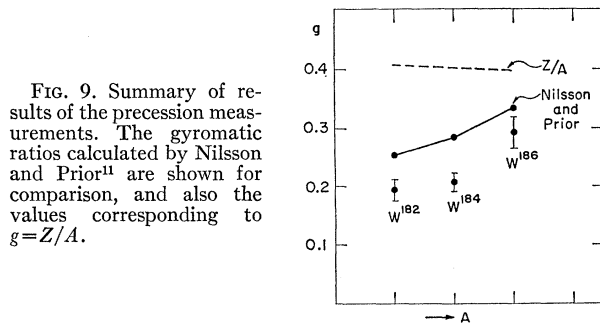


FIG. 9. Summary of results of the precession measurements. The gyromagnetic ratios calculated by Nilsson and Prior¹¹ are shown for comparison, and also the values corresponding to $g = Z/A$.

¹⁰ R. W. Bauer and M. Deutsch, Bull. Am. Phys. Soc. **6**, 224 (1961).

underestimates the true value of ϵ , this cannot be by more than some 30%.

V. RESULTS AND CONCLUSIONS

The results of the g -factor measurements for the 2^+ states of the tungsten isotopes are summarized in Fig. 2. The values corresponding to calculations of Nilsson and Prior¹¹ and values corresponding to $g=Z/A$ are also shown. It is evident that whereas the values measured by Kegel⁴ and Bodenstedt *et al.*⁹ are close to Z/A , the values found in the present measurements are

¹¹ S. G. Nilsson and O. Prior, Kgl. Danske Videnskab. Selskab, Mat.-fys. Medd. **32**, No. 16 (1960).

considerably lower than even the values calculated in reference 11. However, it is interesting to note that the trend of the g factors as a function of A closely follow the predictions of that theory and there is an almost constant ratio of about 0.8 between the measured g factors and those calculated by Nilsson and Prior.

ACKNOWLEDGMENTS

We are greatly indebted to Mrs. Drora Kedem for her devoted help throughout all stages of this work and to Micha Loebenstein for his assistance in programming the computations for the WEIZAC electronic computer. Our thanks are due to H. Brafman for designing and constructing the electronic channeling device.

Excitation of Two-Phonon States by Inelastic α -Particle Scattering

B. BUCK

Oak Ridge National Laboratory,* Oak Ridge, Tennessee

(Received February 19, 1962)

Recent experiments on inelastic scattering of 40-MeV α particles have shown that the angular distributions from the excitation of some known 4^+ states in medium weight nuclei are not in accord with the Blair phase rule. Calculations are reported which indicate that the anomaly arises as an interference effect between two possible mechanisms for exciting the first 4^+ state, i.e., a direct transition and a multiple transition. This conclusion is contrary to previous interpretations based on plane-wave perturbation calculations. It is suggested that experiments of this type, and the analysis given here, promise to be a useful tool for the study of higher excited states.

THE Blair phase rule,^{1,2} for the inelastic scattering of strongly absorbed particles, states that the angular distributions corresponding to even values of the angular momentum transfer L are out of phase with those corresponding to odd- L transfer. Furthermore, the elastic scattering angular distributions should be in phase with the odd- L transfer angular distributions. The conditions for the validity of the phase rule should be adequately fulfilled by 40-MeV (α, α') reactions exciting low-lying collective levels of even-even nuclei. The rule has been extensively verified for the excitation of the lowest 2^+ and 3^- collective states.

Recent experiments^{3,4} have shown that the rule is not obeyed by the inelastic angular distribution of 43-MeV α particles exciting known 4^+ states of nuclei in the nickel region. The experimental distributions for the 4^+

levels are found to be almost exactly out of phase with the 2^+ distributions.

In the vibrational model, the first 4^+ state is interpreted as an excitation containing two quadrupole phonons. Hence, if quadrupole vibrations alone are considered, the state can only be reached by second-order processes. The processes may be calculated if one assumes that the nuclear surface is capable of quadrupole deformations defined by

$$R(\theta, \phi) = R_0 \left[1 + \sum_m \alpha_m Y_2^m(\theta, \phi) \right]. \quad (1)$$

Assuming that the nuclear potential V seen by the α particle depends only on the distance from the surface we have, to second order

$$V(r-R) = V(r-R_0) - \sum_m \alpha_m Y_2^m(\theta, \phi) R_0 \frac{dV}{dr} + \frac{1}{2} \left[\sum_m \alpha_m Y_2^m(\theta, \phi) \right]^2 R_0^2 \frac{d^2V}{dr^2}.$$

The dynamical distortion parameters α_m create or annihilate phonons of angular momentum 2, z component m . $V(r-R_0)$ is taken to be the usual type of

* Operated by Union Carbide Nuclear Company for the U. S. Atomic Energy Commission.

¹ J. S. Blair, Phys. Rev. **115**, 928 (1959).

² E. Rost and N. Austern, Phys. Rev. **120**, 1375 (1960).

³ H. Broek, J. L. Yntema, and B. Zeidman (to be published).

⁴ R. Beurtey, P. Catillon, R. Chaminade, M. Crut, H. Farraggi, A. Papineau, J. Saudinos, and J. Thirion, Compt. rend. **252**, 1756 (1961). The results of references 3 and 4 are also contained in the *Proceedings of the Rutherford Jubilee International Conference, Manchester, 1961* (Academic Press Inc., New York, 1961).